The response of stomatal conductance to vapor pressure deficit over global wheat areas in CMIP6 warming projections

Carlo Montes[1,2], Urs Schulthess[2] and Matthew Reynolds[1]

[1]International Maize and Wheat Improvement Center (CIMMYT), Texcoco, 56237, Mexico

[2]CIMMYT-Henan Collaborative Innovation Center, Henan Agricultural University, Zhengzhou, 450002, China

Corresponding author: Carlo Montes (c.montes@cgiar.org)

Key Points:

- CMIP6 projections show a sustained increase in vapor pressure deficit (VPD) associated with global warming over global wheat areas
- The global response of wheat stomatal conductance (g_s) shows a decreasing trend from around 2040 in the three CMIP6 scenarios evaluated
- The higher sensitivity of g_s to VPD than to air temperature suggests that the areas of decreasing g_s could increase in warmer climates

Abstract

Climate change is expected to alter the conditions in which plants develop. The mechanisms by which plants can adapt to changing conditions must be studied in terms of the magnitude of their response and the implications for productivity. Recognizing wheat as a main crop sustaining global livelihoods as well as the need for long-term adaptation strategies to climate change, this work assesses the response of wheat stomatal conductance (g_s) to changes in vapor pressure deficit (VPD) associated with global warming in three future scenarios from the Coupled Model Inter-comparison Project phase 6 (CMIP6). We used multiple datasets and a modeling approach to estimate g_s as a function of atmospheric variables only over global wheat areas. The results show a sustained increase in both temperature and VPD in the historical period and future CMIP6 scenarios, and a generalized decrease in wheat g_s that becomes clear from around the year 2040. The pattern of change is spatially divergent, with areas that present increases in relation to the historical average, which mostly concentrate towards high latitudes. Negative trends in g_s area mainly observed in North America, Southern Europe, North Africa and Asia. Notwithstanding, the proportion of areas of positive change in g_s tend to decrease in warmer climate scenarios. g_s is more sensitive to changes in VPD than to global warming, which implies that the areas of negative trends in g_s could expand to higher latitudes. These results may assist the regional focus of long-term wheat adaptation programs to climate change.

Plain language summary

Climate change projections are of great relevance for crops, on the one hand due to the increase in temperatures, but also due to the changes in vapor pressure deficit (VPD), an indicator of air dryness. One of the plant responses to changes in temperature and VPD is stomatal closure, which affects transpiration, photosynthesis, and consequently, productivity. This is of great relevance for agricultural crops such as wheat given its importance for global food security. The present study assesses the global response of wheat stomatal conductance (g_s), an indicator of the magnitude of leaf-air gas exchanges, to the changes in VPD under future CMIP6 global warming scenarios. The results show a generalized increase in VPD that is consistent with projected warming over global wheat areas. However, a divergent response in g_s is projected. In general, high latitude areas of both the Northern and Southern hemisphere show an increase in g_s, while lower latitude areas in North America, Asia, and Europe show a decrease in g_s. The results also revealed that the changes in g_s are more sensitive to changes in VPD than to temperature.

1 Introduction

The water losses and CO_2 photosynthetic uptake by plant leaves are controlled by stomatal behavior, which is in turns controlled by biophysical processes counteracting water availability and atmospheric demand (Buckley, 2005). The water flow through the soil-plant-atmosphere continuum is driven by the differences in water potential between the soil and the air surrounding the leaves, locally controlled by leaf transpiration (Passioura, 1982). A higher atmospheric water demand reduces leaf water status, so that the stomata reduce their opening to prevent the decline in water status (Buckley, 2005), playing a key role in the adaptation of plants to changing environmental conditions (Damour et al., 2010). Given the strong relationship between transpired water, crop productivity, and water use efficiency (Miner et al., 2017), the stomatal conductance (g_s), an estimator of the magnitude and dynamics of leaf-air gas exchanges, has been widely used as an indicator of plant water status and as a predictor of yields in crop species such as wheat (Fisher et al., 1998). In this regard, higher yielding wheat varieties have been monitored and described as having higher g_s, consequently lower canopy temperature and heat resistance, thus making g_s useful as a selection metric for high yields under optimal water supply conditions (Lu et al., 1998), and drought tolerance (Bota et al., 2004).

The global observed and projected atmospheric warming leads to an increase in the drying power of air (Broz et al., 2021). This drying effect is driven by the vapor pressure deficit (VPD), the difference between the actual water vapor content (actual vapor pressure) and the maximum amount that the air can hold in the gas phase at a specific temperature (saturated vapor pressure), whose magnitude depends on multiple factors such as land surface evaporation and the large-scale atmospheric environment (Ficklin & Novick, 2017). Increasing attention has been paid to VPD in recent years as its observed increase in the last decades has been associated with a global reduction in vegetation growth (Yuan et al., 2019), offsetting the CO_2 fertilization effect, and with an enhancement of heat stress on crops given its association with land-surface water loss (Lobell et al., 2013). Moreover, anomalously high seasonal values of VPD have been directly associated with the occurrence of droughts (Sanginés de Cárcer et al., 2018). The immediate response of plant to increases in VPD is the stomatal closure, consequently reducing g_s, with impacts on multiple biophysical processes such as evapotranspiration (Grossiord et al., 2020). Plants close their stomata after a certain level of soil water depletion to avoid water loss (Fang et al., 2021) and modern crop varieties are no exception. However, it has been observed that VPD can limit stomatal conductance in a greater extent than soil water content, explaining up to 90% of the variability in g_s in relation to soil moisture in maize and soybean (Kimm et al., 2020), and up to 70% in global croplands and natural ecosystems (Novick et al., 2016). Similarly, VPD has been quantified as the main factor triggering reductions in terrestrial gross primary production (Fu et al., 2022; Lu et al., 2022), and a main driver of plant stress compared with soil water content and available energy (Tong et al., 2019). These studies show that the expected increase in VPD due to climate change could exacerbate stress conditions for crops and terrestrial ecosystems, in addition to the relative importance of atmospheric water demand that could be accentuated under climate change scenarios (Novick et al., 2016).

The current context of climate change poses challenges to global agriculture, especially to field crops such as wheat, given its importance for food security and livelihoods, and the wide range of environments in which wheat is grown (Gbegbelegbe et al., 2017). However, despite the observed increase and robust projections in air temperature and evaporative demand (Byrne & O'Gorman, 2018; Zhu & Troy, 2018; Fang et al., 2022), there is still much uncertainty regarding the projections of rainfall (Sheffield et al., 2012; Shiogama et al., 2022) and therefore on integrating processes such as droughts (Cook et al., 2014) and associated plant responses (Kath et al., 2022). Although VPD is projected to increase in the future as a consequence of the combination of global warming and saturated vapor pressure, changes in actual vapor pressure and relative humidity vary across regions (Byrne & O'Gorman, 2013). The latter results from complex feedback mechanisms that can modify the surface energy partitioning and evaporative fraction (Barkhordarian et al., 2019). Notwithstanding, increases in VPD can exacerbate the water demand and stomatal closure (Damour et al., 2010; Medlyn et al., 2011). Consequently, assessing projected climate conditions acting as drivers of agriculturally relevant hydroclimatic events is necessary to plan long-term adaptation strategies for more water-efficient crop varieties and cropping systems (Damour et al., 2010; Mondal et al., 2020).

Considering the relationship between VPD, stomatal closure and g_s, its consequences on water status of plants, and the role of increasing temperatures, the main objective of this work is to assess the implications that projected changes in VPD associated with global warming would have in terms of climatological g_s trends over global wheat cultivation areas. Although much attention has been paid to the impacts of changes of air temperature and rainfall on wheat and other crops, however, little has been done with respect to the influence of changes in evaporative demand on processes relevant to crop water consumption and productivity. The latter is an important issue for a major staple food for many countries since drought and heat stress are among the most severe factors that reduce wheat productivity. We used outputs from a suite of twenty-first century General Circulation Models (GCMs) simulations issued from the Coupled Model Intercomparison Project phase 6 (CMIP6; Eyring et al., 2016). We calculated g_s with the widely-used Jarvis-type (Jarvis, 1976) multiplicative model, to address the questions on (1) what are the expected changes in VPD associated with global warming over global wheat-producing areas, (2) what might be the expected responses in terms of g_s, and (3) what is the relative importance of changes in temperature and in VPD on the projected g_s. The results from this work represent an assessment of background climate and biophysical conditions affecting wheat physiology that accompany other effects associated with atmospheric composition such as CO_2 fertilization, and can contribute to the identify climate pathways to develop adaptation strategies and provide guidance for wheat breeding.

2 Materials and Methods

2.1 CMIP6 and historical climate datasets

As a primary dataset, we used daily climate data of mean air temperature, downwelling shortwave radiation and relative humidity, from five bias-corrected and downscaled CMIP6 (Eyring et al., 2016) GCMs (Table 1) and three Shared Socioeconomic Pathways (SSP) for the 21st century (SSP126, SSP370 and SP585) at 0.5° × 0.5° spatial resolution. These CMIP6 model outputs belong to the Inter-Sectoral Impact Model Intercomparison Project (ISIMIP, https://www.isimip.org/; Lange and Büchner, 2022). The historical period from 1971 through 2014 was considered, and two future periods: midcentury, from 2041 through 2070, and end of century, from 2071 through 2100.

Table 1. List of CMIP6 GCMs from ISIMIP used in this study.

Model	Institution (country)
GFDL-ESM4	Geophysical Fluid Dynamics Laboratory (United States)
IPSL-CM6A-LR	Institut Pierre-Simon Laplace (France)
MPI-ESM1-2-HR	Max Planck Institute for Meteorology (Germany)
MRI-ESM2-0	Meteorological Research Institute (Japan)
UKESM1-0-LL	Met Office Hadley Centre (United Kingdom)

In addition to CMIP6 projections, we used data from European Centre for Medium-Range Weather Forecasts (ECMWF) AgERA5 product (Copernicus Climate Change Service, C3S, 2019) as an observational reference. AgERA5 corresponds to a statistically downscaled (0.1° × 0.1°) daily time-step version of ERA5 reanalysis. In this case, minimum and maximum air temperature, shortwave radiation and dewpoint temperature data were used, for the period 1981 through 2014. AgERA5 data were resampled to the 0.5º × 0.5º CMIP6 grid resolution using bilinear interpolation.

2.2 Computing vapor pressure deficit

VPD was calculated using the widely used equation of Allen et al. (1998) for water vapor pressure estimation. However, the procedure differs for CMIP6 and AgERA5 data. For CMIP6, saturated vapor pressure (e_s) is computed from air temperature (T) as:

$$e_s = 0.611 \times \exp^{\left(\frac{17.27 \times T}{237.3 + T}\right)}, \quad (1)$$

and actual vapor pressure (e_a) is calculated from relative humidity (RH):

$$e_a = RH \times e_s, \quad (2)$$

with e_s and e_a expressed in kPa, T in ºC, and RH in percentage. VPD is simply calculated as the difference between e_s and e_a:

$$VPD = e_s - e_a. \quad (3)$$

For AgERA5, since dewpoint temperature (T_d; ºC) is available, e_a is calculated as:

$$e_a = 0.611 \times \exp^{\left(\frac{17.27 \times T_d}{237.3 + T_d}\right)}, \quad (4)$$

and VPD is obtained by equation (3).

2.3 Estimating wheat stomatal conductance

We performed a simulation analysis over global wheat areas in order to assess the response of wheat stomatal conductance to global warming and VPD. We calculated stomatal conductance following the widely-used semi-empirical Jarvis analytical formulation, which allows estimating g_s (mol m^{-2} s^{-1}) as the multiplicative effect of environmental factors controlling the relative stomatal closure:

$$g_s = g_{smax} f_1(\mathrm{PAR}) f_2(\mathrm{T}) f_3(\mathrm{VPD}), \quad (5)$$

where g_{smax} is the maximum leaf stomatal conductance when environmental factors are not limiting, in this study set as 0.833 mol m^{-2} s^{-1} (Houshmandfar et al., 2015), f_1, f_2, and f_3 are stress functions representing the influence of independent environmental factor on g_s, which vary between 0 and 1. Following previous studies parameterizing g_s for wheat, the following stress functions were considered:

$$f_1(\mathrm{PAR}) = 1 - \exp(-0.0075 \times \mathrm{PAR}), \quad (6)$$

$$f_2(\mathrm{T}) = 1 - \left(\mathrm{T} - \mathrm{T_{opt}}\right)^2 / \left(\mathrm{T_{opt}} + \mathrm{T_{min}}\right)^2, \quad (7)$$

$$f_3(\mathrm{VPD}) = \frac{1}{1 + \left(\mathrm{VPD}/_{3.75}\right)}, \quad (8)$$

where PAR in Eq. (6) is the incoming photosynthetically active radiation, T in Eq. (7) is the daily mean air temperature, T_{opt} and T_{min} in Eq. (7) are the optimal and minimum temperatures for growth, respectively taken as 23 ºC and 8 ºC. The empirical parameters in the above equations (6) to (8) are taken from previous studies based on field experiments carried out to parameterize the Jarvis model on wheat (Danielsson et al., 2013; Houshmandfar et al., 2015). Recognizing that volumetric soil water content is a relevant variable that is usually incorporated as a stress function in Eq. (5), in this work we assumed well-watered conditions in order to focus only on the impact of atmospheric forcing on g_s. Furthermore, although multiple models exist to calculate stomatal conductance with varying complexity and forcing data requirements (Ball et al., 1987; Leuning, 1990; Tuzet et al., 2003), the Jarvis multiplicative formula corresponds to a meteorological approach that has been implemented in multiple land surface schemes coupled to atmospheric models (Chen & Dudhia, 2001; Xiu & Pleim, 2001; Godfrey & Stensrud, 2010). In the present work, we focused on quantifying the sensitivity of wheat g_s to VPD and warming, so the Jarvis model, which represent the response of g_s to environmental factors, appears to be appropriate.

2.4 Representing wheat area and harvest dates

We obtained global wheat area data from the Spatial Production Allocation Model (SPAM) global crop production product (Yu et al., 2020). This gridded product provides information on harvested area and production for the year 2005 at a spatial resolution of 5-min (0.083º × 0.083º) for multiple crops and is generated by combining information sources about land use and crop production statistics. In this work, SPAM wheat growing area data were initially resampled to the 0.5º × 0.5º CMIP6 grid resolution using bilinear interpolation. In a second step, the resampled data were converted into a binary mask indicating global wheat crop area. SPAM grid cells with a wheat area of less than 5 % were removed. Additionally, global wheat harvest dates for the year 2000 were extracted from the global crop calendar dataset for specific crops of Sacks et al. (2010).

2.5 Analyzes

All the analyzes were performed for the period corresponding to the last 30 days of the wheat growing cycle (as a proxy of the anthesis to maturity period), tanking the harvest dates from Sacks et al. (2010). The mean changes for the 30-year average for the midcentury and end of century periods in relation to the historical average 1971-2014 (CMIP6) and 1981-2014 (AgERA5) were analyzed. Also, the multi-model mean was considered. The first part of the results shows an analysis of the projected changes in VPD in relation to global warming over wheat growing areas. The second part of the results corresponds to the assessment of the implications of changes in VPD and temperature on wheat g_s, which was calculated using the complete historical and future series of VPD, temperature and solar radiation. To quantify the contribution of changes in VPD and temperature on changes in g_s, the influence of VPD and temperature were isolated by calculating g_s for the twentieth century using the detrended VPD (denoted by g_s-*tas*) and temperature (denoted by g_s-*vpd*) of the future periods, and setting the mean of the corresponding time series to be equal to the historical period, as a way to quantify the impact of projected trends of both VPD and temperatures on g_s separately. We excluded solar radiation from this sensitivity analysis to focus on the influence of global warming and VPD trends. This approach has been used in previous studies on the relative contribution of VPD, temperature and radiation to changes in drought indices (Cook et al., 2014; Noguera et al., 2022),

3 Results

3.1 Historical and projected VPD and temperature changes over global wheat areas

Figure 1 shows the historical and projected changes in VPD and air temperature for CMIP6 and AgERA5. A relatively good agreement between the mean CMIP6 changes and AgERA5 is observed, with a Pearson correlation coefficient of 0.64 and 0.72, and a Root Mean Square Error of 0.04 kPa and 0.39 ºC respectively for VPD and temperature. VPD anomalies (obtained by removing the average 1971-2014 and 1981-2014 value for CMIP6 and AgERA5, respectively) over global wheat areas show increasing values that progressively shift to positive from the 1990s in both AgERA5 and CMIP6 (Figure 1a), trends that have been previously highlighted globally (e.g., Yuan et al., 2019; Fang et al., 2022). The latter roughly coincides with the shift from negative to positive anomalies presented by temperature in observations and CMIP6 (Figure 1b). Future projections show a very similar mean evolution until around the year 2040, from which the three future scenarios begin to diverge at an anomaly value of ~0.2 kPa and ~2 ºC, respectively for VPD and temperature (Figure 1a and 1b). Regarding future scenarios, both SSP370 and SSP585 show sustained positive trends until the end of the 21st century, although they start to diverge from around 2040. On the other hand, the SSP126 scenario rather shows an increase until the 2040s to then stabilize at a value close to 0.2 kPa and 2 ºC in VPD and temperature, respectively. Trends in actual values are presented in Figure S1 in Supporting Information S1.

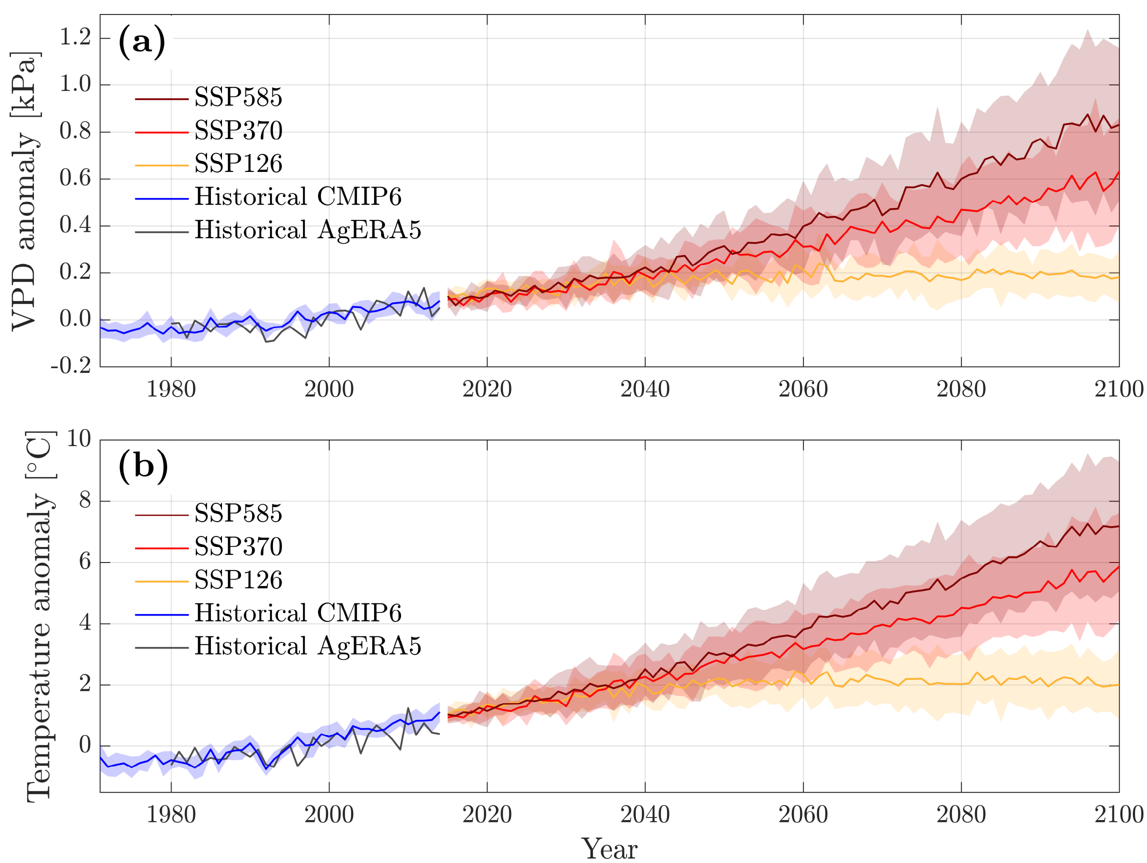

Figure 1. Time series of historical and projected (a) VPD and (b) air temperature anomalies over global wheat areas. Solid lines are the multi-model mean, and the shaded area represent the spatial standard deviation. Calculations are made for the 30 days wheat heading periods.

The scatter plot of the relationship between the change in VPD and global warming over global wheat areas is presented in Figure 2, which shows the global mean values for each CMIP6 scenarios and GCMs. According to these results, global warming is expected to increase VPD in a slightly exponential relationship that is well captured by an exponential factor of 1.23 (Figure 2). The low-end SSP126 scenario, which was generated to analyze the response of the climate system to declining greenhouse gasses emissions, shows an average increase in VPD of up to 0.4 kPa in warmer climates. The magnitude of these changes is comparable to what has been observed historically in both CMIP6 and observations (Figure 1), suggesting that agricultural and natural systems could respond in a similar way to what has been observed in recent decades (Yuan et al., 2019). The SSP370 and SSP585 scenarios are associated with higher levels of warming, with values typically above 2 ºC in warmer climates (Figure 2). Considering reference global warming values of 2 ºC and 4 ºC, Figure 2 shows an increase in VPD between 0.2 and 0.4 kPa on average, which is relatively high in relation to the historical average of 1.1 kPa over wheat areas (Figure S2 in Supporting Information S2).

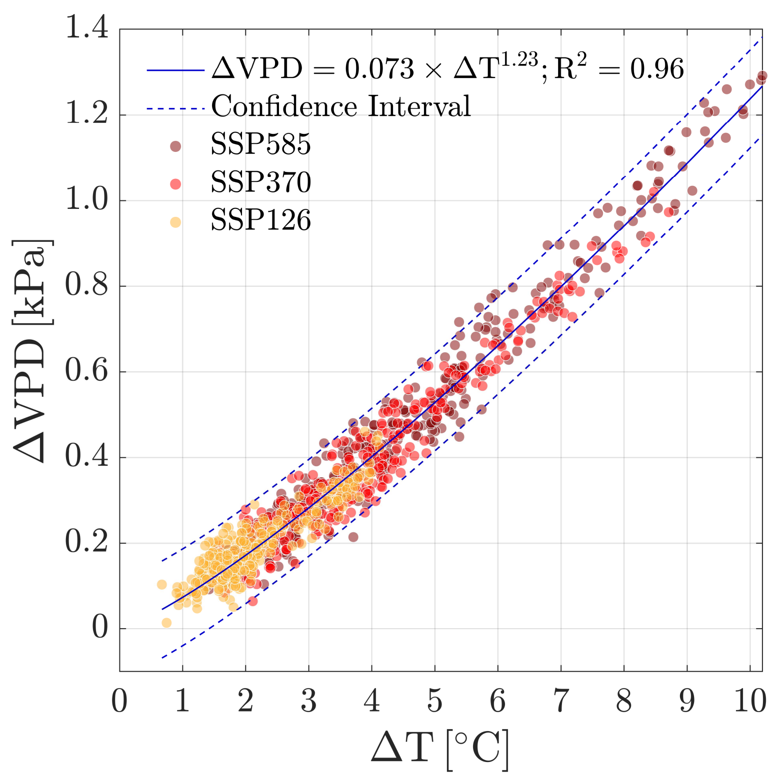

Figure 2. Scatter plot between global annual change (Δ) in VPD and annual mean warming (ΔT) over global wheat areas for the three CMIP6 scenarios and periods (2041-2100). Each dot represents the mean value from the five GCMs used (n = 900). The continuous line corresponds to the exponential fit, and dashed lines bound the 95% confidence interval. The equation of the exponential fit is also displayed.

The climatology of projected changes in VPD in relation to global mean warming over wheat areas for multi-model mean, CMIP6 scenarios and future periods are presented in Figure 3. The spatial patterns of VPD change look similar for the three CMIP6 scenarios and future time windows (midcentury and end of century). Maximum VPD increases range between 0.32 kPa/ºC and 0.36 kPa/ºC, with higher values mostly concentrated towards lower latitudes in Southern Europe, Asia and North America, areas in which pronounced trends in VPD are projected (Figure S3 in Supporting Information S3). Lower values are observed over areas such as South America, South Asia and Southern Africa. Clearly, the mean values close to 0.1 kPa/ºC found across scenarios is associated with the similar rate of increase of both VPD and temperature (Figure 1). Thus, based on these results, it can be inferred that the sensitivity of the change in VPD is about 0.1 kPa per degree Celsius of change in temperature.

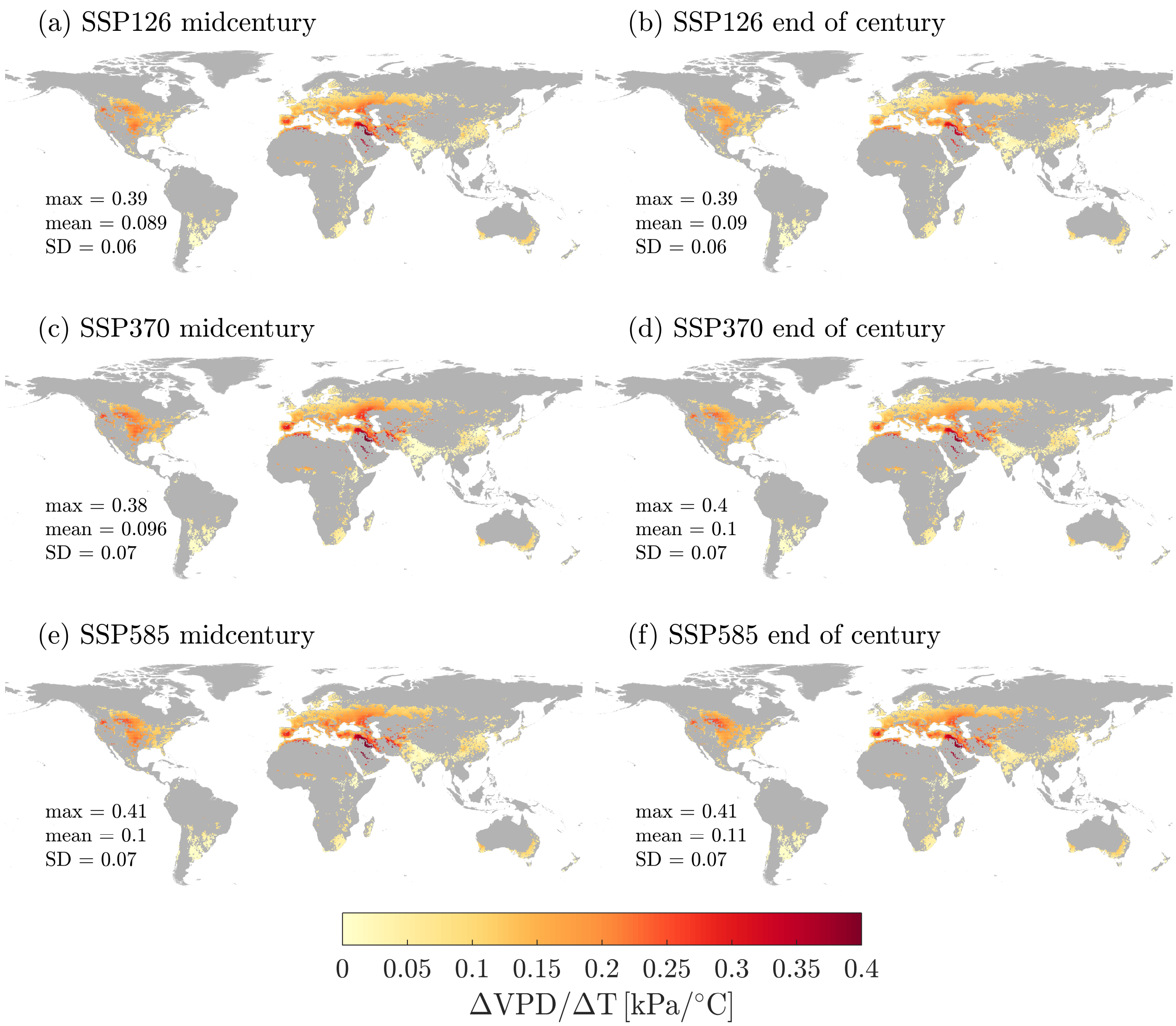

Figure 3. Maps of change in VPD per degree of warming (ΔVPD/ΔT) over global wheat areas for multi-model midcentury (2041-2070) and end of century (2071-2100) means and for the three CMIP6 scenarios. The maximum, mean and standard deviation (SD) are also displayed.

3.2 Wheat stomatal conductance and global warming

The response of g_s to changes in VPD and temperature are presented in this section. The main patterns in projections are summarized in Figure 4, which shows the scatter plot of the relationship between future g_s, expressed as relative to the maximum value (g_s/g_{smax}), and the change in VPD and temperature. Similar to Figure 2, the global mean values for each CMIP6 scenario and GCM are displayed. Figure 4a shows a sharp decrease at increasing rates of g_s as a function of VPD in future climates, suggesting a continuous decrease in g_s as global warming drives higher rates of changes in VPD. Similarly, the relationship between g_s and temperature shows a strong drop in g_s as global scenarios become warmer, similar to VPD (Figure 3a). However, in the case of temperature, there seems to be a global warming level that generates a positive response in g_s, concentrated in the SSP126 scenarios, which represents a stabilization in the global temperature at a level close to 2 ºC from around the year 2040 in relation to the historical average 1971-2014 (Figure 1). On the contrary, the scenarios of a sustained increase in temperature at a rate similar to recent decades for the midcentury period are characterized by a sustained decrease g_s, up to values close to 25% (i.e., g_s/g_{smax} = -0.25).

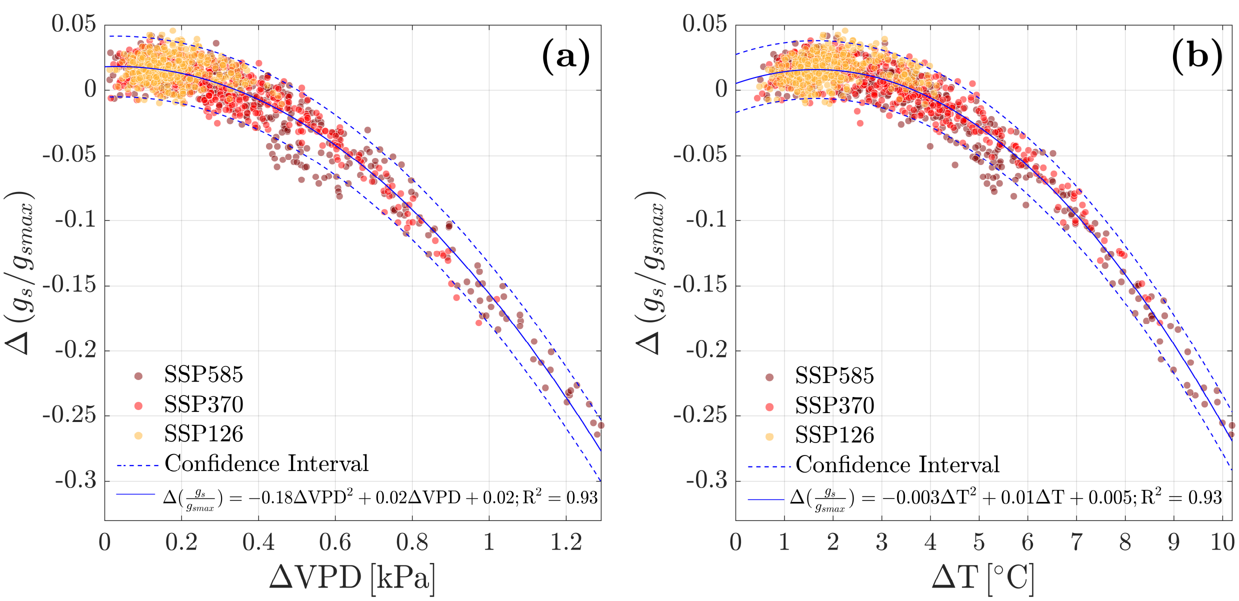

Figure 4. Scatter plot between global annual change (Δ) in g_s relative to the maximum value (g_s/g_{smax}) and (a) mean VPD and (b) temperature (T) over global wheat areas for the three CMIP6 scenarios and periods (2041-2100). Each dot represents the mean value from the five GCMs used (n = 900). The continuous line corresponds to the polynomial fit, and dashed lines bound the 95% confidence interval. The equation of the second-degree polynomial fit is also displayed.

The future climatology of g_s for midcentury and end of century periods and scenarios show a spatial distribution of positive and negative values of g_s/g_{smax} (Figure 5). For the three scenarios, median values remain close to zero from midcentury to the end of the century, but higher positive and negative changes are observed. In general, increases in g_s are observed at high latitudes of the Northern and Southern Hemisphere, and a reduction in g_s over lower latitudes areas of North America, Europe, and Asia, which is coincident with the areas of greater increase in both VPD (Figure 3) and temperature (Figure S4 in Supporting Information S4). Australia appears as the only country in the Southern Hemisphere that shows dominant decreasing g_s. In addition, the maps of Figure 5 show an increasing/decreasing relative area of negative/positive changes in g_s as climate becomes warmer. In this way, while the SSP126 scenario presents a very slight temporary change from midcentury or end of century (Figure 5a and 5b), both SSP370 and SSP585 scenarios represent a dominant area of negative changes in g_s that increases in time (Figure 5c-5f). The latter is evidenced, for example, in the expansion of negative changes in g_s/g_{smax} values over Southern Europe and in South Asia.

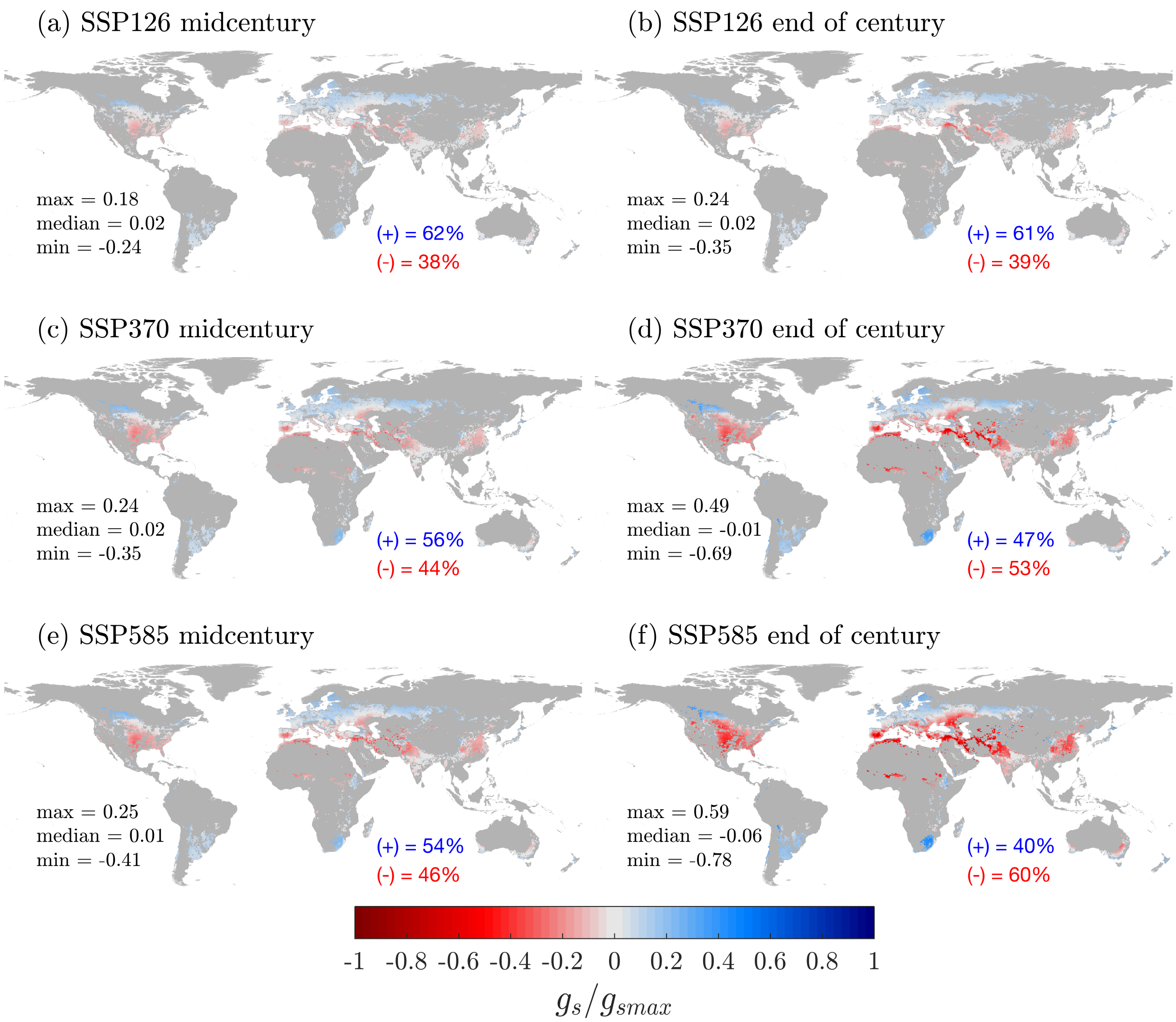

Figure 5. Multi-model mean g_s relative to the maximum value (g_s/g_{smax}) over global wheat areas for midcentury (2041-2070) and end of century (2071-2100) and for the three CMIP6 scenarios. The maximum, median and minimum (SD) are displayed, as well as the percentage area with positive and negative changes.

3.3 Sensitivity of wheat stomatal conductance to vapor pressure deficit and temperature

The maps of projected changes in g_s after detrending VPD and setting the mean value to the historical 30-day wheat grain filling period (g_s-*tas*) are displayed in Figure 6, where a spatially contrasting response in terms of positive and negative changes in g_s/g_{smax} is observed. This diverging pattern is similar to that obtained by including both VPD and temperature (Figure 5), with an increase in g_s at high latitudes in the Northern and Southern hemispheres, and a negative response at low latitudes that concentrate in the Northern Hemisphere. In terms of values, differences between scenarios and future period (midcentury and end of century) are low, which range between -0.8 and 0.4 in the most extreme means. Nevertheless, a decrease/increase in the proportion of positive/negative changes appears again as a clear pattern that differentiates future scenarios. Additionally, the maps of Figure 6 and Figure 5 show a similar spatial distribution of g_s/g_{smax}, although the higher magnitudes in negative changes. On the other hand, sensitivity of g_s to changes VPD isolating the effect of temperature (g_s-*vpd*), presented in Figure 7, show a remarkable expansion of the areas with negative changes in g_s, with the exception of a small area in high latitudes of the Northern and Southern hemispheres. A particular feature of g_s-*vpd* is the spatially uniform and similarity of the median and extreme values for the three future scenarios and two climatological periods, along with the proportion of positive and negative changes.

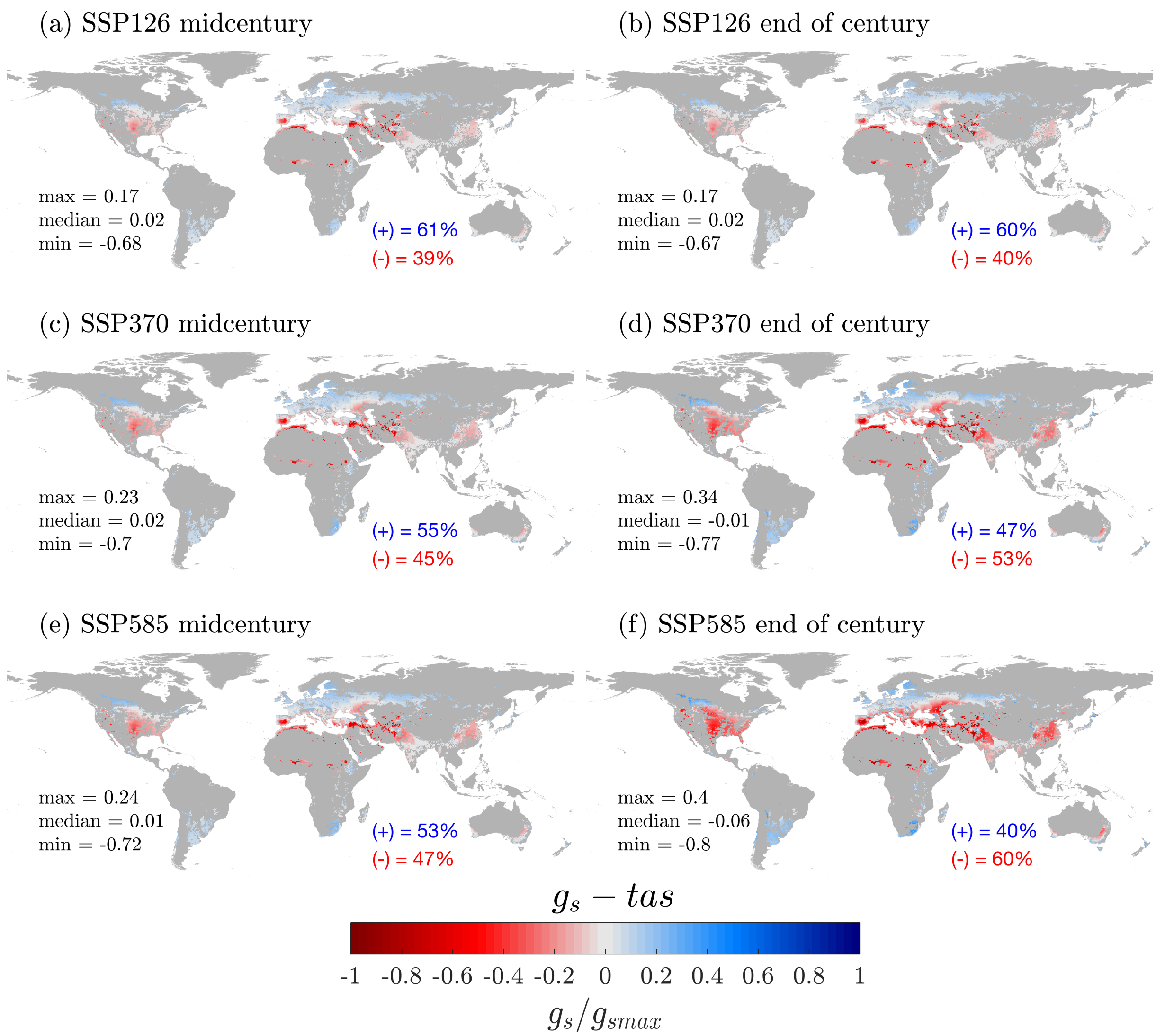

Figure 6. Multi-model mean g_s-tas relative to the maximum value (g_s/g_{smax}) over global wheat areas for midcentury (2041-2070) and end of century (2071-2100) and for the three CMIP6 scenarios. The maximum, median and minimum (SD) are displayed, as well as the percentage area with positive and negative anomalies.

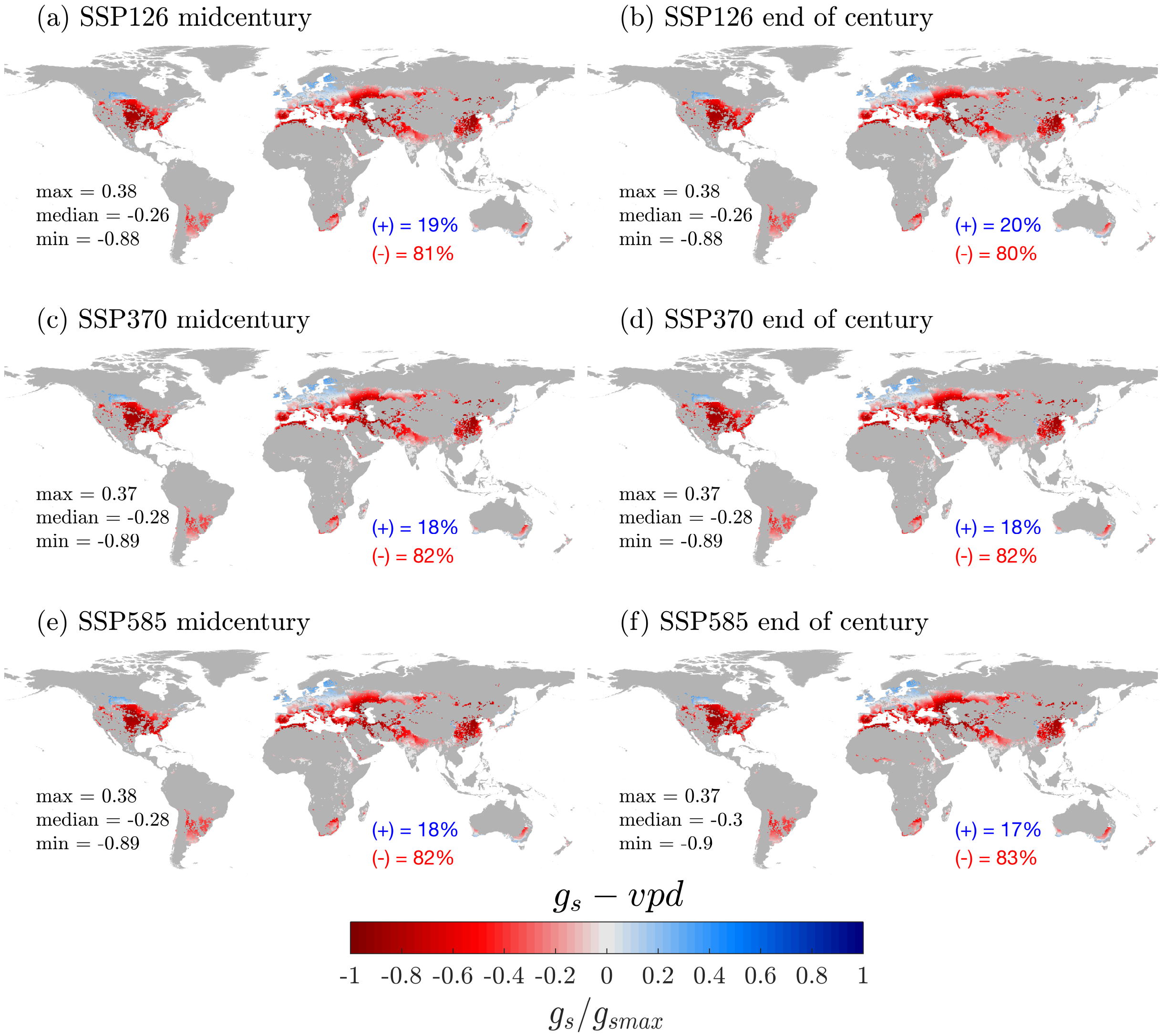

Figure 7. Multi-model mean g_s-vpd relative to the maximum value (g_s/g_{smax}) over global wheat areas for midcentury (2041-2070) and end of century (2071-2100) and for the three CMIP6 scenarios. The maximum, median and minimum (SD) are displayed, as well as the percentage area with positive and negative anomalies.

The above-presented results are summarized in Figure 8, where the mean g_s/g_{smax} obtained from the three CMIP6 scenarios are presented as zonal averages of the difference between the future (2041-2100) and historical (1971-2014) periods. First, the difference between the g_s response between the Northern and Southern hemispheres is clear, associated with the difference in wheat area. In general, in the case of g_s calculated using both VPD and temperature (*gs-all* in Figure 8), g_s decreases from northern high latitudes towards more tropical latitudes, shifting from positive to negative changes from around 50 ºN to then become positive generally from around 10 ºN and in the Southern hemisphere, evidencing a contrasting response. The curve of g_s removing the effect of VPD (g_s-*tas*) looks similar to that of g_s-*all*, except for a band of large drop in g_s near 30 ºN-40 ºN, which more or less corresponds to North America, Southern Europe, North Africa, Central Asia, as well as a region close to 10 ºN-15 ºN, represented mainly by the

North of the Sub-Saharan Africa (Figure 6). In contrast, the curve of differences for the case of sensitivity to VPD (g_s-*vpd*) is more pronounced in terms of the decrease with respect to g_s-*all*. In this case, the change from positive to negative anomalies in the Northern Hemisphere is more abrupt, remaining negative throughout all latitudes, except for a small latitudinal band between about 10 ºN and 20 ºN. In the Southern Hemisphere, while both g_s-*all* and g_s-*tas* represent an increase in g_s, g_s-*vpd* remains negative.

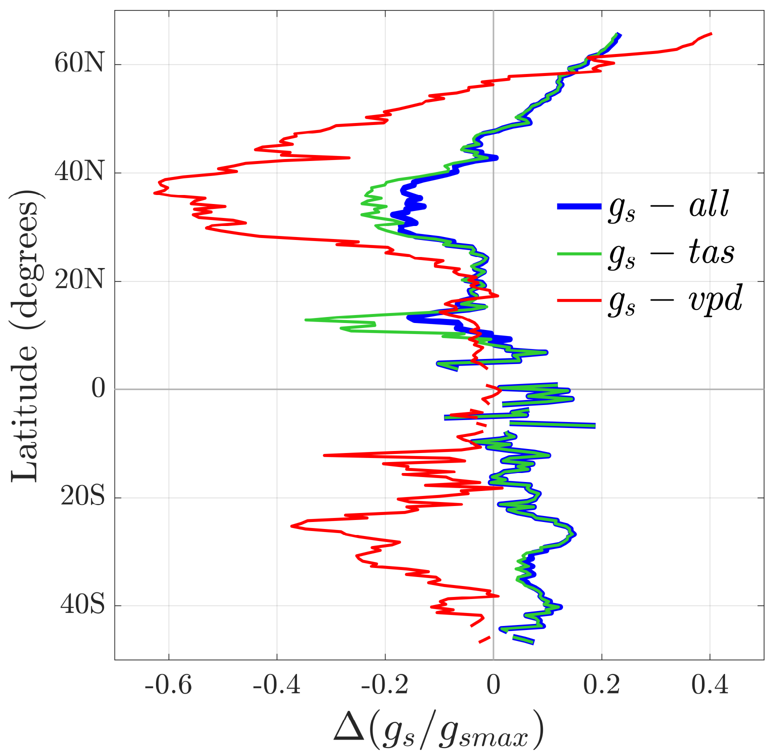

Figure 8. Zonally averaged multi-model and scenario mean g_s/g_{smax} (2041–2100). g_s-all (Figure 5), g_s-tas (Figure 6) and g_s-vpd (Figure 7).

4 Discussion

4.1 Global warming, VPD, and wheat stomatal conductance

By focusing on the climatological aspects related with global warming and the associated increasing in atmospheric water demand, which has become evident in recent decades, the main goal of this work is the assessment of the possible future trajectories in VPD and global warming over global wheat areas, and their implications for g_s. The results represent an overview of the potential background conditions associated with climate change to which wheat cultivation could be subjected in the coming decades. Although trends in the drying power of the air, represented by VPD, has been characterized (Fang et al., 2022) and found as controlling water cycle and limiting plant growth globally (Zhang et al., 2015; Yuan et al., 2019), no specific studies has focused on staple crops such as wheat. The data- and modeling-based results suggest a steady increase in historical and projected VPD over global wheat areas that is very consistent with temperature projections, except for SSP126 which represents a stabilization in both VPD and temperature from around 2040. The reasons for this increase can be attributed to the increase in temperature and consequently in the saturated vapor pressure, and a decrease in actual vapor pressure, for example, over areas with negative in trends rainfall, such as North America (Seager et al., 2015) or South America (Barkhordarian et al., 2019), or globally as a result of the global depletion in soil moisture (Deng et al., 2020). However, this increase in VPD is more pronounced over areas such as Southern Europe, Northern Africa and Central Asia, which could be considered as hotspots of increasing evaporative demand (Ficklin & Novick, 2017) and associated consequences on stress conditions (Grossiord et al., 2020) enhanced by higher temperatures (Hatfield & Prueger, 2015). Furthermore, taking VPD 3 kPa as a global reference value above which transpiration rate is affected (Tamang et al., 2022), CMIP6 projections show a significant increase in the number of days exceeding 3 kPa during the last 30 days of the wheat growing cycle (Figure S5 in Supporting Information S5).

The global response of g_s to CMIP6 projections in VPD and warming shows an exponential decay in g_s (Figure 4). It is worthwhile commenting that this corresponds to a climatological relationship that differs from the inverse and nonlinear relationship often found in field measurements of g_s and VPD, where a drop in g_s with an asymptotic convergence to a certain minimum value of g_s is observed (e.g., Grossiord et al., 2020). Notwithstanding, the previously-presented results in terms of VPD and temperatures show a diverging spatial response of g_s (Figure 5), which suggests that some regions of the global wheat production area would benefit from climate change in terms of the response in g_s. The foregoing provided that water supply is assured, which is very unlikely to happen in areas of projected decrease in rainfall, higher drought conditions and water demand (Cook et al., 2014). Howevet, the results show a dominant increasing trend in negative changes in g_s, which represents adverse conditions for wheat cultivation given the limitations to transpiration and photosynthetic rate of lower g_s (Sperry et al., 2016), as well as the soil moisture depletion and drought effects of high VPD (Farahmand et al., 2021). In this sense, irrigated areas could need greater access to irrigation infrastructure, and rainfed areas would most likely suffer from water stress and lower yields (Zhou et al., 2019). On the other hand, cross-year effects could occur due to low g_s in drier regions, over which soil moisture could remain in the soil for the next wheat growing season. In this way, advances in water conservation technologies (e.g., irrigation, conservation tillage) in addition to cultivars with different sensitivity to VPD could help to increase adaptation capacitates. Although multiple studies have quantified the fertilization effect of the higher atmospheric CO_2 concentrations (e.g., Degener, 2015), which could help to offset the effect of the lower g_s, its effect on wheat could be very low or even null under water stress conditions partly due to changes in stomatal traits (Zheng et al., 2020).

The sensitivity of g_s to changes in VPD and temperature reveals the relevance that increasing atmospheric water demand may have in the future, as it has been highlighted in recent years (Yuan et al., 2019). The latter is evidenced in the proportion of the global wheat area that responds positively to changes in temperature (Figure 6), versus the negative changes in g_s when considering trends in VPD only (Figure 7), as well as the sustained decrease in g_s in global averages (Figure S6 and S7 in Supporting Information S6 and S7, respectively). These results highlight the importance of considering suitable parameterizations of g_s and water stress effects in terms of their response to changes in VPD in current crop and terrestrial biosphere models in order to have realistic estimates of the possible trajectories in crop response to changing climate. However, these findings should in the future be supported by regional observations on the relationship between VPD and wheat physiology, as it has been done previously for the case of corn, where minor effects of increasing VPD and potential evapotranspiration on yields have been projected in North America (Basso et al., 2021; Riha & Melkonian, 2022;)

4.2 Uncertainties and limitations

The main data source for this study corresponds to the state-of-the-art CMIP6 climate projections. However, we used a modeling approach and a combination of datasets that have associated multiple sources of uncertainty. For instance, we used the Jarvis multiplicative model of g_s, which allows to easily isolate the effect of changing VPD and in temperature on g_s, using specific parameters for wheat. Although the incorporation of other processes such as carbon uptake and photosynthesis or the effect of soil moisture, which can be carried out with the Jarvis or others models, would help to further analyze the potential response of g_s to climate change. However, this is out of the scope of this work since we focus only on the response to VPD in relation to global warming.

We used secondary information as boundary conditions and assumptions in terms of wheat cropping calendars and phenology, which represents an important source of uncertainty and limitations since we have tried to project the ecophysiological response of wheat to future climate scenarios based on wheat phenology, among other information. For instance, we used fixed harvest dates from Sacks et al. (2010), which are naturally variable from year to year. Similarly, the SPAM for wheat area representation corresponds to a static product that might over- and under-estimate the wheat cultivation area (Montes et al., 2022). The latter becomes delicate when assuming that, for example, wheat development and phenology should also be affected by global warming (Jägermeyr et al., 2021). However, our approach seeks at providing insights of the possible long-term future trajectories that wheat cultivation could be heading, assuming the deep uncertainty existing when it comes to climate change. Fortunately, genetic variation in response of g_s to VPD has been observed in wheat (Tamang et al., 2022) and other crops.

5 Conclusions

Global warming is expected to alter the functioning of agro-ecosystems in many ways. One of them is in the magnitude of gas exchanges between plants and the atmosphere, which can be quantified by stomatal conductance (g_s). The aim of this work was to assess the possible future climate scenarios in terms of the magnitude in which g_s could be affected, representing a challenge for wheat cultivation given the implications on water use and stress. Our results show a significant increase in both temperatures and VPD over global wheat areas, which represents, *per se*, a threat to wheat cultivation since VPD is a well-known driver of drought-related stresses on crops. Regarding the projected response of g_s to both global warming and VPD, our results suggest a differential response ranging from negative to positive climatological multi-model anomalies for the three scenarios considered (SSP126, SSP370, SSP585) across wheat cultivation areas. The contrasting response of g_s, with positive changes over high-latitude areas versus negative changes in lower latitude areas of the Northern Hemisphere, may be indicative of a relative benefit of higher temperatures over some areas, which was evidenced in the temperature sensitivity analysis (g_s-*tas*; Figure 6). However, the progressive decrease of the area with positive anomalies in g_s as the climate becomes warmer suggest that this effect could be offset. In addition, the clear negative effect of VPD on g_s should alert about possible climate change scenarios for wheat, and in turn could assist in the design and development of long-term adaptation strategies. In this way, efforts could focus on the use of soil moisture conservation techniques and development of new wheat varieties adapted to conditions of high atmospheric water demand and drought over those areas with higher changes in g_s such as in Asia and Norther Africa, where drought-related stress conditions (Cook et al., 2014) could be exacerbated by atmospheric factors limiting g_s. The latter is supported by our results highlighting the trends in VPD and its importance for wheat g_s. Accordingly, future efforts in understanding the response of g_s to VPD in historical observational data and modeling would allow for a better interpretation on how g_s could respond to future climate scenarios, and in this way to incorporate more biophysical processes in the analyzes. Such results can be used to refine breeding targets so that, for example, a cultivar's response of gs to VPD suits a particular water-deficit profile considering VPD and other environmental factors.

Acknowledgments

This work was supported by the CGIAR Foresight initiative (https://www.cgiar.org/initiative/foresight/) and the CGIAR Digital Innovation initiative (https://www.cgiar.org/initiative/digital-innovation/).

Data Availability Statement

All the GCMs and boundary conditions data sets used in this study are publicly available and can be accessed from the original references provided in the text. The archiving process of the historical and projected VPD and stomatal conductance data sets for global wheat areas is underway.

References

Allen, R. G., Pereira, L. S., Raes, D., & Smith, M. (1998), Crop evapotranspiration. Guidelines for computing crop water requirements. FAO Irrigation and drainage paper 56, FAO, Rome, 300, 6541, 1998.

Ball, J. T., Woodrow, I. E., & Berry, J. A. (1987), A model predicting stomatal conductance and its contribution to the control of photosynthesis under different environmental conditions. In: Progress in Photosynthesis Research. Springer, pp. 221-224, https://doi.org/10.1007/978-94-017-0519-6_48

Barkhordarian, A., Saatchi, S. S., Behrangi, A., Loikith, P. C., & Mechoso, C. R. (2019), A recent systematic increase in vapor pressure deficit over tropical South America. *Scientific Reports.* 9, 15331. https://doi.org/10.1038/s41598-019-51857-8

Basso, B., Martinez-Feria, R.A., Rill, L., & Ritchie, J.Y. (2021), Contrasting long-term temperature trends reveal minor changes in projected potential evapotranspiration in the US Midwest. *Nature Communications*. 12, 1476. https://doi.org/10.1038/s41467-021-21763-7

Tamang, B.G., Monnens, D., Anderson, J.A, Steffenson, B.J., and Sadok, W. (2022), The genetic basis of transpiration sensitivity to vapor pressure deficit in wheat. *Physiologia Plantarun*. 174:e13752. https://doi.org/10.1111/ppl.13752

Bota, J., Medrano, H., & Flexas, J. (2004), Is photosynthesis limited by decreased Rubisco activity and RuBP content under progressive water stress?. *New Phytologist*. 162, 671-681. https://doi.org/10.1111/j.1469-8137.2004.01056.x

Broz, A., Retallack, G.J., Maxwell, T.M., & Silva, L.C.R. (2021), A record of vapour pressure deficit preserved in wood and soil across biomes. *Scientific Reports*. 11, 662. https://doi.org/10.1038/s41598-020-80006-9

Buckley, T.N. (2005), The control of stomata by water balance. *New Phytologist*. 168, 275-291. https://doi.org/10.1111/j.1469-8137.2005.01543.x

Byrne, M.P., & O'Gorman, P.A. (2018), Trends in continental temperature and humidity directly linked to ocean warming. *Proceedings of the National Academy of Science*. 115, 4863-4868. https://doi.org/10.1073/pnas.1722312115

Chen, F., & Dudhia, J. (2001), Coupling an advanced land-surface/hydrology model with the Penn state/NCAR MM5 modeling system. Part I: model description and implementation. *Monthly Weather Review*. 129, 569-585, https://doi.org/10.1175/1520-0493(2001)129<0569:CAALSH>2.0.CO;2

Damour, G., Simonneau, T., Cochard, H., & Urban, L. (2010), An overview of models of stomatal conductance at the leaf level. *Plant, Cell and Environment*. 33, 1419-1438. https://doi.org/10.1111/j.1365-3040.2010.02181.x

Cook, B.I., Smerdon, J.E., Seager, R., & Coats, S. (2014), Global warming and 21st century drying. *Climate Dynamics*. 43, 2607-2627. https://doi.org/10.1007/s00382-014-2075-y

Copernicus Climate Change Service (C3S). (2019), Data Stream 2: AgERA5 historic and near real time forcing data. Product User Guide and Specification. Copernicus Climate Change Service Climate Data Store (CDS). Online: http://datastore.copernicus-climate.eu/documents/sis-global-agriculture/C3S422Lot1.WEnR.DS2_ProductUserGuideSpecification_v2.2.pdf

Danielsson, H., Karlsson, G. P., Karlsson, P. E., & Pleijel, H. (2003), Ozone uptake modelling and flux-response relationships - an assessment of ozone-induced yield loss in spring wheat. *Atmospheric Environment*. 37, 475-485. https://doi.org/10.1016/S1352-2310(02)00924-X

Degener, J.F. (2015), Atmospheric CO_2 fertilization effects on biomass yields of 10 crops in northern Germany. *Frontiers in Environmental Science*, 3:48. doi:10.3389/fenvs.2015.00048

Deng, Y., Wang, S., Bai, X., Luo, G., Wu, L., Cao, Y., Huiwen, L., Chajun, L., Yang, Y., Hu, Z., & Tian. S. (2020), Variation trend of global soil moisture and its cause analysis. *Ecological Indicators*. 110, 105939. https://doi.org/10.1016/j.ecolind.2019.105939

Eyring, V., Bony, S., Meehl, G. A., Senior, C. A., Stevens, B., Stouffer, R. J., & Taylor, K. E. (2016), Overview of the Coupled Model Intercomparison Project Phase 6 (CMIP6) experimental design and organization. *Geoscientific Model Development.* 9(5), 1937-1958. https://doi.org/10.5194/gmd-9-1937-2016

Fang, Y. L., Leung, L. R., Wolfe, B. T., Detto, M., Knox, R. G., McDowell, N. G., Grossiord, C., Chonggang, X., Christoffersen, B.O., Gentine, P., Koven, C.D., & Chambers, J.Q. (2021), Disentangling the effects of vapor pressure deficit and soil water availability on canopy conductance in a seasonal tropical forest during the 2015 El Nino drought. *Journal of Geophysical Research: Atmospheres*, 126(10), e2021JD035004. https://doi.org/10.1029/2021JD035004

Fang, Z., Zhang, W., Brandt, M., Abdi, A.M., & Fensholt, R. (2022), Globally increasing atmospheric aridity over the 21st century. *Earth's Future*. 10, e2022EF003019. https://doi.org/10.1029/2022EF003019

Farahmand, A., Reager, J. T., & Madani, N. (2021), Drought cascade in the terrestrial water cycle: Evidence from remote sensing. *Geophysical Research Letters*, 48(14), e2021GL093482. https://doi.org/10.1029/2021gl093482

Ficklin, D. L., & Novick, K. A. (2017), Historic and projected changes in vapor pressure deficit suggest a continental scale drying of the United States atmosphere. *Journal of Geophysical Research-Atmosphere*. 122, 2061-2079. https://doi.org/10.1002/2016JD025855

Fischer, R.A., Rees, D., Sayre, K.D., Lu, Z.-M., Condon, A.G., & Saavedra, A.L. (1998), Wheat yield progress associated with higher stomatal conductance and photosynthetic rate, and cooler canopies. *Crop Science*. 38: 1467-1475. https://doi.org/10.2135/cropsci1998.0011183X003800060011x

Fu, Z., Ciais, P., Prentice, I.C., Gentine, P., Makowski, D., Bastos, A., Luo, X., Green, J.K., Stoy, P.C., Yang, H., & Hajima T. (2022), Atmospheric dryness reduces photosynthesis along a large range of soil water deficits. *Nature Communications*. 13, 989. https://doi.org/10.1038/s41467-022-28652-7

Gbegbelegbe, S., , Cammarano, D., Asseng, S., Robertson, R., Chung, U., Adam, M., Abdalla, O., Payne, T., Reynolds, M., Sonder, K., Shiferaw, B., & Nelson, G. (2017), Baseline simulation for global wheat production with CIMMYT mega-environment specific cultivars. *Field Crops Research*. 202, 122-135. https://doi.org/10.1016/j.fcr.2016.06.010

Godfrey, C. M., & Stensrud, D. J. (2010), An empirical latent heat flux parameterization for the Noah Land Surface Model. *Journal of Applied Meteorology Climatology*. 49, 1696-1713, https://doi.org/10.1175/2010JAMC2180.1

Grossiord, C., Buckley, T. N., Cernusak, L. A., Novick, K. A., Poulter, B., Siegwolf, R. T. W., Sperry, J. S., & McDowell, N. G. (2020), Plant responses to rising vapor pressure deficit. *New Phytologist*. 226, 1550-1566. https://doi.org/10.1111/nph.16485

Hatfield, J. L., & Prueger, J. H. (2015), Temperature extremes: effect on plant growth and development. *Weather and Climate Extremes*. 10, 4-10, https://doi.org/10.1016/j.wace.2015.08.001.

Houshmandfar, A., Fitzgerald, G. J., Armstrong, R., Macabuhay, A. A., & Tausz, M. (2015), Modelling stomatal conductance of wheat: an assessment of response relationships under elevated CO_2. *Agricultural and Forest Meteorology*. 214-215, 117-123, https://doi.org/10.1016/j.agrformet.2015.08.249

Jarvis, P. G. (1976), The interpretation of leaf water potential and stomatal conductance found in canopies in the field. *Philosophical Transactions of the Royal Society of London B*. 273, 593-610. https://doi.org/10.1098/rstb.1976.0035

Jägermeyr, J., and coauthors. (2021), Climate impacts on global agriculture emerge earlier in new generation of climate and crop models. *Nature Food*, 2, 873-885. https://doi.org/10.1038/s43016-021-00400-y

Kath, J., Craparo, A., Fong, Y., Byrareddy, V., Davis, A.P., King, R., Nguyen-Huy, T., van Asten, P.J.A., Marcussen, T., Mushtaq, S., Stone, R., & Power, S. (2022), Vapour pressure deficit determines critical thresholds for global coffee production under climate change. *Nature Food*. 3, 871-880. https://doi.org/10.1038/s43016-022-00614-8

Kimm, H., Guan, K., Gentine, P., Wu, J., Bernacchi, C. J., Sultan, B. N., Griffis, T. J., & Lin, C. (2020), Redefining droughts for the U.S. Corn Belt: the dominant role of atmospheric vapor pressure deficit over soil moisture in regulating stomatal behavior of Maize and Soybean. *Agricultural and Forest Meteorology*. 287, 107930. https://doi.org/10.1016/j.agrformet.2020.107930

Lange, S., & Büchner, M. (2022), Secondary ISIMIP3b bias-adjusted atmospheric climate input data (v1.0). ISIMIP Repository. https://doi.org/10.48364/ISIMIP.581124

Leuning, R. (1990), Modelling stomatal behaviour and photosynthesis of Eucalyptus grandis. *Australian Journal of Plant Physiology*. 17, 159. https://doi.org/10.1071/pp9900159

Lobell, D. B., Hammer, G. L., McLean, G., Messina, C., Roberts, M. J., & Schlenker, W. (2013), The critical role of extreme heat for maize production in the United States. *Nature Climate Change*. 3, 497-501. https://doi.org/10.1038/nclimate1832

Lu, Z., Percy, R.G., Qualset, C.O., & Zeiger, E. (1998), Stomatal conductance predicts yields in irrigated Pima cotton and bread wheat grown at high temperatures. *Journal of Experimental Botany*. 49, 453-460. https://doi.org/10.1093/jxb/49.Special_Issue.453

Lu, H., Qin, Z., Lin, S., Chen, X., Chen, B., He, B., Wei, J., & Yuan, W. (2022), Large influence of atmospheric vapor pressure deficit on ecosystem production efficiency. *Nature Communications*. 13, 1653. https://doi.org/10.1038/s41467-022-29009-w

Medlyn, B.E., Duursma, R.A., Eamus, D., Ellsworth, D.S., Prentice, I.C., Barton, C.V.M., Crous, K.Y., De Angelis, P., Freeman, M., & Wingate, L. (2011), Reconciling the optimal and empirical approaches to modelling stomatal conductance. *Global Change Biology*. 17, 2134-2144. https://doi.org/10.1111/j.1365-2486.2010.02375.x

Miner, G.L., Bauerle, W. L., & Baldocchi, D. D. (2017), Estimating the sensitivity of stomatal conductance to photosynthesis: a review. *Plant, Cell and Environment*. 40, 1214-1238, https://doi.org/10.1111/pce.12871.

Mondal, S., Dutta, S., Crespo-Herrera, L., Huerta-Espino, J., Braun, H.J., & Singh, R. P. (2020), Fifty years of semi-dwarf spring wheat breeding at CIMMYT: grain yield progress in optimum, drought and heat stress environments. *Field Crops Research*. 250, 107757. https://doi.org/10.1016/j.fcr.2020.107757

Montes, C., Hussain, S.G. & Krupnik, T.J. (2022), Variable climate suitability for wheat blast (Magnaporthe oryzae pathotype Triticum) in Asia: results from a continental-scale modeling approach. *International Journal of Biometeorology*. 66, 2237-2249. https://doi.org/10.1007/s00484-022-02352-9

Noguera, I.,Vicente-Serrano, S. M., & Domínguez-Castro, F. (2022), The rise of atmospheric evaporative demand is increasing flash droughts in Spain during the warm season. *Geophysical Research Letters*. 49, e2021GL097703. https://doi.org/10.1029/2021GL097703

Novick, K. A., Ficklin, D. L., Stoy, P. C., Williams, C. A., Bohrer, G., Oishi, A. C., Papuga, S. A., Blanken, P. D., Noormets, A., Sulman, B. N., Scott, R. L., Wang, L., and Phillips, R. P. (2016), The increasing importance of atmospheric demand for ecosystem water and carbon fluxes. *Nature Climate Change*. 6, 1023-1027, https://doi.org/10.1038/nclimate3114

Passioura, J.B. (1982), Water in the soil-plant-atmosphere continuum. In: Lange, O.L., Nobel, P.S., Osmond, C.B., Ziegler, H. (eds) Physiological Plant Ecology II. Encyclopedia of Plant Physiology, vol 12/B. Springer, Berlin, Heidelberg.

Riha, S., & Melkonian, J. (2022), Limited impact of vapor pressure deficit on rainfed maize evapotranspiration, CO_2 flux, and canopy temperature. *Agronomy Journal*. 00, 1-15. https://doi.org/10.1002/agj2.21254

Sacks, W. J., Deryng, D., Foley, J. A., & Ramankutty, N. (2010), Crop planting dates: an analysis of global patterns. *Global Ecology and Biogeography*. 19, 607-620, https://doi.org/10.1111/j.1466-8238.2010.00551.x

Sanginés de Cárcer, P., Vitasse, Y., Penuelas, J., Jassey, V. E. J., Buttler, A., & Signarbieux, C. (2018), Vapor-pressure deficit and extreme climatic variables limit tree growth. *Global Change Biology*. 24, 1108-1122. https://doi.org/10.1111/gcb.13973

Seager, R., Hooks, A., Williams, A. P., Cook, B., Nakamura, J., & Henderson, N. (2015), Climatology, variability, and trends in the U.S. vapor pressure deficit, an important fire-related meteorological quantity. *Journal of Applied Meteorology and Climatology*. 54, 1121-1141, https://doi.org/10.1175/JAMC-D-14-0321.1

Sheffield, J., Wood, E.F., 6 Roderick, M.L. (2012), Little change in global drought over the past 60 years. Nature 491, 435-438. https://doi.org/10.1038/nature11575

Shiogama, H., Watanabe, M., Kim, H., & Hirota, N. (2022), Emergent constraints on future precipitation changes. *Nature*. 602, 612-616. https://doi.org/10.1038/s41586-021-04310-8.

Sperry, J. S., Wang, Y., Wolfe, B. T., Mackay, D. S., Anderegg, W. R., McDowell, N. G., & Pockman, W. T. (2016), Pragmatic hydraulic theory predicts stomatal responses to climatic water deficits. *New Phytologist*. 212, 577-589. https://doi: 10.1111/nph.14059

Tong, X., Mu, Y., Zhang, J., Meng, P., & Lu, J. (2019), Water stress controls on carbon flux and water use efficiency in a warm temperate mixed plantation. *Journal of Hydrology*. 571, 669-678, https://doi.org/10.1016/j.jhydrol.2019.02.014

Tuzet, A., Perrier, A., & Leuning, R. (2003), A coupled model of stomatal conductance, photosynthesis and transpiration. *Plant, Cell and Environment*. 26, 1097-1116, https://doi.org/10.1046/j.1365-3040.2003.01035.x

Xiu, A., & Pleim, J. E. (2001), Development of a land surface model. Part I: Application in a mesoscale meteorological model. *Journal of Applied Meteorology*. 40, 192-209, https://doi.org/10.1175/1520-0450(2001)040<0192:DOALSM>2.0.CO;2

Yu, Q., You, L., Wood-Sichra, U., Ru, Y., Joglekar, A. K. B., Fritz, S., Xiong, W., Lu, M., Wu, W., & Yang, P. (2020), A cultivated planet in 2010 - part 2: the global gridded agricultural-production maps, *Earth System Science Data,* 12, 3545-3572. https://doi.org/10.5194/essd-12-3545-2020

Yuan, W., and coauthors. (2019), Increased atmospheric vapor pressure deficit reduces global vegetation growth. *Science Advances*, 5: eaax1396. DOI: 10.1126/sciadv.aax1396

Zhang, K., Kimball, J. S., Nemani, R. R., Running, S. W., Hong, Y., Gourley, J. J., & Yu, Z. (2015), Vegetation greening and climate change promote multidecadal rises of global land evapotranspiration. *Scientific Reports*. 5, 15956. https://doi.org/10.1038/srep15956

Zheng, Y., He, Ch., Guo, L., Hao, L., Cheng, D., Li, F., Peng, Z., & Xu, M. (2020), Soil water status triggers CO_2 fertilization effect on the growth of winter wheat (*Triticum aestivum*). *Agricultural and Forest Meteorology*, 291, 108097. https://doi.org/10.1016/j.agrformet.2020.108097

Zhou, S., Zhang, Y., Williams, A. P., & Gentine, P. (2019), Projected increases in intensity, frequency, and terrestrial carbon costs of compound drought and aridity events. *Science Advances*, 5(1), eaau5740. https://doi.org/10.1126/sciadv.aau5740

Zhu, X., & Troy, T.J. (2018), Agriculturally relevant climate extremes and their trends in the world's major growing regions. *Earth's Future*, 6, 656-672. https://doi.org/10.1002/2017EF000687